EUROPEAN JOURNAL OF ENTOMOLOGY
ISSN (online): 1802-8829
http://www.eje.cz
Eur. J. Entomol. **123**: 208–216, 2026
doi: 10.14411/eje.2026.021
ORIGINAL ARTICLE

Electrophysiological response of *Pentastiridius leporinus* (Hemiptera: Cixiidae) to plant volatiles and the ultrastructure of its antennal sensilla

Eva Therhaag[1,2], Katja R. Richert-Pöggeler[3], Verena Maiberg[3], Natascha Heil[4] and Jürgen Gross[1,2]

[1] Julius Kühn Institute (JKI) – Federal Research Centre for Cultivated Plants, Institute for Plant Protection in Fruit Crops and Viticulture, Schwabenheimer Str. 101, 69221 Dossenheim, Germany; e-mails: eva.therhaag@julius-kuehn.de, juergen.gross@julius-kuehn.de

[2] Hochschule Geisenheim University, Department of Crop Protection, Von-Lade-Str. 1, 65366 Geisenheim, Germany

[3] Julius Kühn Institute (JKI) – Federal Research Centre for Cultivated Plants, Institute for Epidemiology and Pathogen Diagnostics, Messeweg 11–12, 38104 Braunschweig, Germany; e-mails: katja.richert-poeggeler@julius.kuehn.de, verena.maiberg@julius-kuehn.de

[4] Julius Kühn Institute (JKI) – Federal Research Centre for Cultivated Plants, Institute for Biological Control, Schwabenheimer Str. 101, 69221 Dossenheim, Germany; e-mail: natascha.heil@julius-kuehn.de

Key words. GC-EAD, EAG, scanning electron microscopy (SEM), transmission electron microscopy (TEM), *Solanum bulbocastanum*

Abstract. The planthopper *Pentastiridius leporinus* transmits the phytoplasma '*Candidatus* Phytoplasma solani' and the bacterium '*Candidatus* Arsenophonus phytopathogenicus' to various agricultural crops and vegetables, mainly in Germany and neighbouring countries. We collected headspace volatiles from the wild potato species *Solanum bulbocastanum* and tested antennal responses of *P. leporinus* using gas-chromatography-electroantennographic detection (GC-EAD). Two identified compounds, nonanal and decanal, were then tested on female antennae using electroantennography (EAG). Both compounds elicited significant dose-dependent EAG responses. Scanning electron microscopy revealed three sensillum types on the pedicel (chaetica, campaniform-like, plate-organs) of both female and male specimens. Transmission electron microscopy showed two coeloconic sensilla inside the Bourgoin organ in ultrathin antennal sections of a female. This is the first report of electrophysiologically active plant volatiles and antennal ultrastructure for this vector.

INTRODUCTION

Pentastiridius leporinus (Linnaeus, 1761) is an emerging insect pest that transmits obligate biotrophic plant pathogens, namely the Stolbur phytoplasma '*Candidatus* Phytoplasma solani', including its P-strain (Duduk et al., 2023), and the γ-proteobacterium '*Candidatus* Arsenophonus phytopathogenicus' (Sémétey et al., 2007), to a wide range of crops such as sugar beet, potato, onion, carrot and other vegetables (Behrmann et al., 2023; Therhaag et al., 2024a, b; Lang et al., 2025; Witczak et al., 2026, 2025). Infested plants often show discolouration of leaves, lower yields or a complete loss due to poor harvest quality (Lang et al., 2025; Mahillon et al., 2025). Furthermore, the Stolbur phytoplasma is a regulated non-quarantine pathogen in potato with 0% tolerance for seed potatoes defined by the European and Mediterranean Plant Protection Organization (EPPO, 2023). As a consequence, the area of seed potato production decreased drastically in the hot spot region in southern Hesse, from 306 ha ± 16.8 ha (mean ± SD, 2017–2021) to 64 ha in 2025 (Landesbetrieb Landwirtschaft Hessen, pers. inform. 2026).

So far, little is known about volatile organic compounds (VOCs), which may be attractive or repellent to *P. leporinus*. Previous mortality experiments showed lethal effects of the wild potato *Solanum bulbocastanum* (Dunal, 1814) on *P. leporinus*, and, surprisingly, a choice test revealed preference of this insect for the wild potato (Therhaag et al., 2026). To test our hypothesis that VOCs are involved in eliciting this behaviour, we collected VOCs from *S. bulbocastanum* and recorded the electrophysiological response of the planthopper antennae in GC-EAD experiments. Two of three electrophysiologically active VOCs were identified using coupled gas chromatography and mass spectrometry (GC-MS), and subjected to an EAG experiment. We also investigated the surface and ultrastructure of antennal sensilla of *P. leporinus* using scanning electron microscopy (SEM) and transmission electron microscopy (TEM). Both the electrophysiological response and ultrastructure of the

antennae are reported here for this planthopper species for the first time.

MATERIAL AND METHODS

2.1 Plants

Single tubers of *S. bulbocastanum* (a clonal line 'blb2G', kindly provided by Julius Kühn Institute (JKI), Berlin, Germany) were planted and grown as described by Lenz et al. (2025), and later sent to JKI Dossenheim, and there transferred to 3 L pots filled with potting soil to sand in a ratio of 4 : 1 (v/v) in an insect-free greenhouse. The environmental conditions were maintained at an average temperature of 23°C and a relative humidity of 40% during the day and 60% at night. During Central European Time (winter time), supplemental artificial lighting was provided to achieve a daily light intensity of 120 klux, otherwise daylight was used.

2.2 Insects

For the GC-EAD experiments, adult females of the planthopper *P. leporinus*, field-caught on 17 July 2025 in Bingen, Germany (49°57′01.8″N, 7°56′05.8″E), and, due to limited field catches, adult males from rearing (JKI Dossenheim, generation F2) were used. No sex-specific differences in EAD responses were assumed. Female adults of *P. leporinus* from rearing (JKI Dossenheim, generation F14) were taken for the electroantennography experiments. For scanning electron microscopy, adult male and female planthoppers from both the F2 and F14 rearing generations were analysed. For the transmission electron microscopy, we used male and female adult planthoppers caught in-field on 2 July 2025 in Wiesbaden, Germany (50°2′12.5484″N, 8°20′35.43′E).

2.3 Collection of volatiles

Volatiles from single shoots of *S. bulbocastanum* (n = 6, biological replicates) were collected before flowering, on 2 and 23 May 2025 in the greenhouse at the JKI, Dossenheim, Germany with an advanced headspace collection device (FLUSYS GmbH, Offenbach, Germany), described by Karimi & Gross (2024). Charcoal-filtered air was passed through Teflon tubes inserted into plastic oven bags (Melitta Group Management GmbH & Co. KG, Minden, Germany) that were pre-conditioned at 60°C for 4 h and cooled before use. Volatiles of one shoot per bag were then trapped in connected pre-conditioned, stainless-steel tubes filled with Tenax TA (35/60 mesh) (Markes, Neu-Isenburg, Germany) at a flow rate of 1 L/min, for 30 min. Sampled tubes were stored in a glass container at room temperature before GC-MS analysis or GC-EAD. At each sampling date, headspace volatiles were collected three times consecutively per plant, with one empty-bag control per date.

2.4 Analysis of volatiles

Volatiles collected in stainless-steel tubes were analysed using a thermal desorber (ATD 650, PerkinElmer, Rodgau, Germany) connected to a gas chromatograph (Clarus 680, PerkinElmer, Rodgau, Germany) coupled with a mass spectrometer (Clarus 600S, PerkinElmer, Rodgau, Germany) (TD-GC-MS).

Three sample tubes (each from a different plant) were desorbed for 10 min at 250°C, with the cold trap held at −20°C continuously, then heated at 99 K/s to 250°C and held for 1 min. The flow of the volatile compounds was split to a ratio of 30 : 70, so that 30% of the flow was transferred via a transfer line into a non-polar Elite-5MS capillary column of 30 m × 0.25 mm inner diameter × 0.25 µm film thickness (Crossbond 5% diphenyl – 95% dimethyl polysiloxane, PerkinElmer, Rodgau, Germany) for separation, and further mass detection using a quadrupole inert mass detector (600 S, PerkinElmer, Rodgau, Germany). Helium was used as carrier gas (5.0, Linde, Munich, Germany) at 130 kPa with a flow rate of 1 mL/min. GC settings were: oven initial temperature of 40°C for 1 min, then heated from 50 to 180°C at 10 K/min (hold for 0 s) and finally increased to the final temperature of 280°C by a rate of 20 K/min (hold for 6 min); with a GC inlet line temperature of 250°C, and the ion source set to 180°C, and a total run time of 26 min. The quadrupole mass detector operated at 70 eV ionisation energy and the full-scan mass spectra were within the range of 50 to 350 m/z.

Compounds eliciting antennal response during the GC-EAD were analysed using the AMDIS software (Automated Mass Spectral Deconvolution and Identification System, V. 2.73, National Institute of Standards and Technology NIST, USA) as previously described by Gross et al. (2019) with settings as in Therhaag et al. (2026). Ion fragmentation patterns, retention times (RT) and retention indices (RI) of these compounds were compared to matches of the NIST library (National Institute of Standards and Technology), and to standard compounds of our in-house library that were introduced in the same system.

2.5 Gas chromatography coupled electroantennographic detection

Collected volatiles of *S. bulbocastanum* were subjected to thermodesorption and gas chromatography coupled electroantennographic and flame ionisation detection (TD-GC-FID/EAD). First, volatiles captured in stainless-steel tubes were desorbed in a thermodesorber (TD 300, PerkinElmer, Rodgau, Germany) as described for the TD-GC-MS, then transferred to a gas chromatograph (GC, Clarus 680, PerkinElmer, Rodgau, Germany) equipped with a flame ionisation detector (FID). Transfer line and settings for both the TD and GC, were equal to the TD-GC-MS. Helium (5.0, Linde, Munich, Germany) was chosen as carrier and auxiliary gas. The volatile flow was injected splitless into a four-port splitter (SilFlow® GC 4 port splitter, Trajan Scientific Europe Ltd, Milton Keynes, UK) as recommended by the manufacturer for this U-shaped arrangement of the ports (Product Data Sheet – SilFlow® GC 4 port splitter, 2022). Here, a stream of auxiliary gas (5 mL/min) carried the compounds eluting from the GC over to the port connected to the FID, and finally to the port for electroantennographic detection (EAD). The effluent for the EAD was passed through a heated transfer line (280°C, Syntech Temperature Controller, Kirchzarten, Germany) into a customised L-shaped glass tube (8 mm inner and 10 mm outer diameter, Seele Glasapparatebau & Laborservice, Rheinbach, Germany) with continuous, charcoal-filtered and humidified air stream (0.12 L/min) directed towards the insect antenna.

For the antenna preparation, the head of the planthopper was mounted onto a custom-pulled glass capillary containing the indifferent, reference electrode and Ringer's solution as described in Syntech (2004), Rid et al. (2019), and Faal et al. (2023). The tip of the antenna was cut to improve electrical contact. It was inserted into another custom-pulled glass capillary with the recording electrode, also filled with Ringer's solution. In both glass capillaries, silver wires were used as electrodes. The analogue signal was detected with an EAG combi probe (INR-II, Ockenfels Syntech GmbH, Buchenbach, Germany), captured and processed with a data acquisition controller (IDAC-2, Syntech, Hilversum, The Netherlands). Recordings of FID and EAD signals were triggered by the GC effluent, analysed and displayed with GcEad 2014 v.1.2.5 software (Syntech, Kirchzarten, Germany). EAD signals corresponding to FID peaks were averaged and defined as alterations of the antennal baseline. Only non-disrupted antennal signals were selected for analysis. Corresponding FID peaks were matched by RI and RT of the GC-MS chromatograms for

identification of those compounds eliciting electrophysiological antennal response. Antennal physiological activity and integrity were verified by applying puffs of a positive control substance (hexane, 5 µl at 0.25 L/min) before and at the end of a run. GC-EAD experiments were conducted using headspace samples of shoots of *S. bulbocastanum* on antennal preparations from adult males ($n = 11$) and females ($n = 13$).

2.6 Electroantennography

Female planthoppers of *P. leporinus* were subject to electroantennography (EAG) testing of ascending concentrations of two single plant compounds. For this, nonanal (purity ≥95%, Sigma Aldrich Chemie GmbH, Taufkirchen, Germany) and decanal (purity ≥99%, Sigma Aldrich Chemie GmbH, Taufkirchen, Germany) were diluted in methanol to obtain tenfold dilution series from 1 to 0.0001 (v/v). Antenna preparation was equal to those of the GC-EAD experiments. A constant flow of charcoal-filtered and humidified air (0.12 L/min) was passed over the prepared antenna through the open end of the L-shaped glass tube, as described for the GC-EAD.

The testing compound (1 µl) was applied on a piece of filter paper inserted in a glass pipette. Using a stimulus controller (CS-55, Syntech, Hilversum, The Netherlands), the pulse duration of the puff was set to 0.1 s at a pulse flow of 0.25 L/min. An interval time of 60 s between puffs was chosen, as well as two replicate stimuli per concentration. The same methanol that was used as a solvent was also used as solvent control (1 µl) and applied before and after each tested compound concentration. Stimuli of ambient air and methanol (1 µl) were applied before and at the end of each compound testing row as negative control and for correction purposes. Hexane (1 µl) was used as a positive control because of its known non-specific antennal activity in preliminary tests. This allowed for later normalisation of the response signal. In total, five antennae from five different females were used per concentration, and each antenna was tested with all concentrations in ascending order. EAG responses were recorded with the EAGPro software (v 2.0, 2015, Syntech, Kirchzarten, Germany).

2.7 Scanning electron microscopy (SEM)

For scanning electron microscopy, we used three different approaches to prepare and analyse the samples (Bozzola, 2014; Richert-Pöggeler et al., 2019).

In the first approach, intact and naturally deceased adult female and male specimens of *P. leporinus* ($n = 2$, one of each sex) from rearing were mounted on a specimen holder using conductive carbon adhesive pads (Plano GmbH, Wetzlar, Germany). After coating with a 22.5 nm layer of gold using the sputter coater K500X (Quorum Technologies, Laughton, UK) they were investigated with a SEM Quanta250 (FEI Deutschland GmbH, Dreieich, Germany) equipped with a tungsten filament. Images obtained under low vacuum conditions at 70 Pa and 20 kV, with a large-field detector (LFD) were scanned at 12 µs with a resolution of 2048×1768 (Griffin, 2007). We applied this method for Fig. 3A.

For the second set of samples, intact, adult female and male specimens of *P. leporinus* ($n = 5$, of each sex) were briefly anaesthetised with CO_2 and directly placed inside the microscope, which led to their death. Afterwards, the samples were treated and investigated as specified above without gold coating. This method was applied for Fig. 3B.

In the third approach, intact, adult female and male specimens of *P. leporinus* ($n = 4$, two of each sex) were killed by CO_2 asphyxiation and immediately dehydrated before electron microscopy (Bozzola, 2014). After replacing water in the samples stepwise with ethanol (30%, 50%, 70%, 80%, 90%, 96%), they were critical point dried (CPD) using the EM CPD300 (Leica Mikrosysteme GmbH, Vienna, Austria). After mounting the insects on the specimen holder and coating with gold as specified above, specimens were investigated in high vacuum at 20 kV, using an Everhart-Thornley detector (ETD). Images were obtained with 10 µs scan speed and a resolution of 1024×884. This method was applied for Fig. 3C–F and Fig. 4A.

The first method (gold coating, low vacuum) gave Fig. 3A, the second method (no coating) Fig. 3B, and the third method (dehydration, CPD) gave Fig. 3C–F and 4A.

2.8 Transmission electron microscopy (TEM)

For the transmission electron microscopy, heads with antennae of intact, adult female and male specimens of *P. leporinus* ($n = 10$, of each sex) were detached from the insect body using a scalpel after a brief anaesthesia with CO_2. Immediately after, they were immersed in a solution of Karnovsky's fixative (2.5% glutaraldehyde and 2% paraformaldehyde in 0.1 M cacodylate buffer, pH 7.4) and 5% sucrose and kept at 4°C for 20 h. The next steps contained the following modifications from the protocol of Romani et al. (2009): specimens were rinsed three times for 1 h in 0.1 M sodium cacodylate buffer containing 5% sucrose and post-fixed in 2% OsO_4 (osmium tetroxide) in the same buffer for 1.5 h. After washing again in 0.1 M cacodylate buffer three times, the specimens were kept at 4°C overnight in 70% ethanol.

To enhance contrast, the samples were stained with 0.5% uranyl acetate in 70% ethanol for 2 h. Following the dehydration process in a graded ethanol series, the samples were embedded in Spurr resin (Spurr low viscosity embedding kit, Sigma Aldrich/Merck KGaA, Darmstadt, Germany) using propylene oxide as a bridging solvent.

Thin sections of 50–70 nm from three distinct antennae were produced using an ultramicrotome (PowerTome XL, RMC Products by Boeckeler Instruments, Inc., Tucson, USA) and mounted on formvar-coated 200-mesh grids. Mounted ultrathin sections were stained at room temperature with uranyl acetate for 10 min, followed by 3% lead citrate for 2 min. A Zeiss EM 900 transmission electron microscope, operated at 80 kV, was used for sample investigation. A total of 13 grids containing sections from one antenna each of a male (2 grids) and a female specimen (11 grids) were examined. Images were captured with a slow-scan, side-mounted 2K CCD camera (TRS Tröndle Restlichtverstärkersysteme, Moorenwies, Germany) and processed using Image SP software (SYSPROG & TrS, Minsk, Belarus).

2.9 Statistical analysis

Statistical analysis was only done for the electroantennography (EAG) experiments.

In case of diluted compounds, EAG responses were corrected by subtracting the response elicited by the solvent (mean of two subsequent replicates) from the response elicited by the tested compound (mean of two subsequent replicates). The response to air (mean of replicates at the beginning and at the end of each concentration row) was maintained for diluted compounds, for consistency. To account for possible olfactory adaptation or physiological degradation of the antenna during the recording, the values were divided by the response elicited by the positive control (the mean of replicates at the beginning and at the end of each concentration row), which resulted in relative EAG responses and normalised units (calculation amended from Ren et al., 2017). In case of undiluted compounds, neither solvent nor air response was subtracted. Statistical analysis was performed on the relative EAG responses, using R version 4.6.0 (R Core Team, 2026). To account for the repeated-measures design (multiple concentrations and stimuli tested on the same individuals), a Linear Mixed Model (LMM) using the 'lmerTest' package (Kuznet-

sova et al., 2026) was employed. The relative antennal response was modelled as a fixed effect of the interaction between stimulus and concentration (treated as a combined grouping factor), while individual insect identity was included as a random intercept to control for baseline sensitivity variations between preparations.

The significance of the overall model was assessed using a Type III ANOVA with Satterthwaite's method for approximating degrees of freedom. Following a significant global effect, post-hoc comparisons were conducted using Dunnett's test in the 'emmeans' package (Lenth et al., 2026) with Kenward-Roger degrees of freedom to compare each stimulus-concentration group against the respective control (methanol and/or air).

Model assumptions were verified by visual inspection of residual Q-Q plots and confirmed by a Shapiro-Wilk test ($W = 0.98$, $p = 0.33$), indicating no significant deviation from normality. Homoscedasticity was confirmed by plotting residuals against fitted values. All reported p-values are adjusted for multiple comparisons using the Dunnett method. Data and underlying R code are made available (https://doi.org/10.5073/20260421-161521-0).

RESULTS

3.1 GC-MS analysis

In this study, we focused on those plant volatiles from *S. bulbocastanum* which elicited an electrophysiological response from the antennal preparation of the planthopper *P. leporinus*. A more in-depth study of the headspace collected volatile organic compounds from this plant species was undertaken recently by Therhaag et al. (2026). Three compounds elicited an electrophysiological response from antennal preparations; one of these could not be reliably identified. Two of them, nonanal (RI 1104) and decanal (RI 1206), could be identified and confirmed with standard compounds of the in-house library at the JKI in Dossenheim, Germany. A third, unidentified compound also elicited a reproducible EAD response but did not match any library spectrum or standard. The third EAD-active compound (unidentified) is not discussed further.

3.2 GC-EAD experiments

For the GC-EAD experiments, eight out of eleven antennal preparations from adult male planthoppers remained attached during the GC run. Their signals recorded by electroantennodetection, as well as the signals from the flame ionisation detector, were subjected to averaging and resulted in three signals corresponding to peaks (Fig. 1), of which two could be identified by GC-MS, namely nonanal (RI 1104) and decanal (RI 1206).

Only five of thirteen antennal preparations of female specimens remained stable in the glass capillaries throughout the entire GC run, and thus were selected for analysis. No reproducible EAD responses above baseline were recorded from any female preparation (n = 13).

3.3 EAG experiments

As the GC-EAD setup did not show reliable alterations of the antennal baseline of female *P. leporinus* to the GC effluent, the two identified compounds, nonanal and decanal, for the male antennae were tested in a more direct manner, via EAG, on antennae of female specimens.

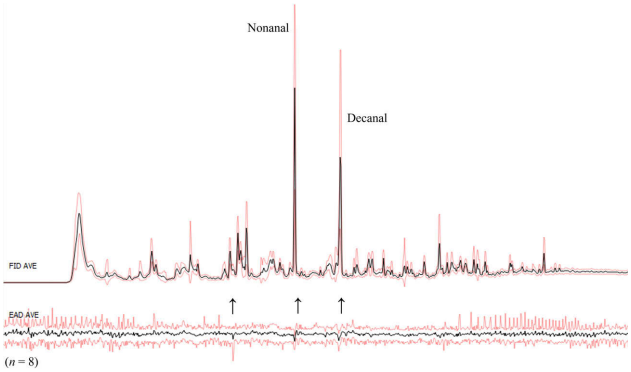

Fig. 1. Displayed are the first 22 min of the GC run (in total 26 min). Black curves are averaged signals of eight recordings of the flame ionisation detector (FID) and the electroantennographic detection (EAD), the standard deviation of both is shown in red curves. Arrows point from EAD signals to peaks of the FID chromatogram.

Statistical analysis revealed that EAG responses (normalised to the hexane standard, estimated mean ± SE) were significantly affected by the stimulus-concentration group (LMM, Type III ANOVA, $F_{12,63} = 30.65$, $p < 0.001$). The random effect of 'insect identity' accounted for a variance of 0.005, representing approximately 2.1% of the total model variance. Post-hoc comparisons (Dunnett's test) revealed that significant activation above the air control level occurred at the highest concentration (1.0) for both compounds, with nonanal eliciting the most pronounced response with 0.647 ± 0.07 (normalised units, $p < 0.0001$), compared to decanal with 0.329 ± 0.07 (normalised units, $p = 0.0001$). At lower concentrations, only nonanal elicited significant responses at 0.1 ($p < 0.0001$) and 0.01 ($p = 0.016$) with 0.442 ± 0.07 and 0.2285 ± 0.07, respectively (normalised units), Fig. 2. No significant difference was observed between the air control and the solvent methanol

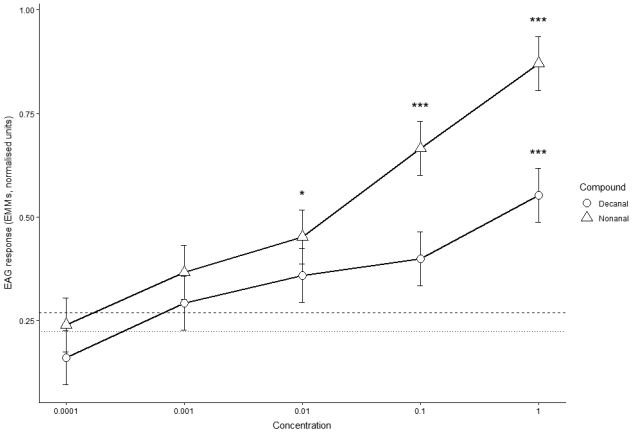

Fig. 2. Relative EAG response data (normalised units) from female *P. leporinus* (*n* = 5) to ascending concentrations of decanal and nonanal. Data points represent estimated marginal means (EMMs) ± standard error derived from a linear mixed model with individual as a random effect; circles: decanal; triangles: nonanal; dotted line: air control; dashed line: solvent (methanol). Asterisks indicate significant responses compared to air after multiple comparisons using Dunnett's test with Kenward-Roger degrees-of-freedom adjustment of p-values; with '*' for $p < 0.05$ and '***' for $p < 0.001$ (95% confidence intervals).

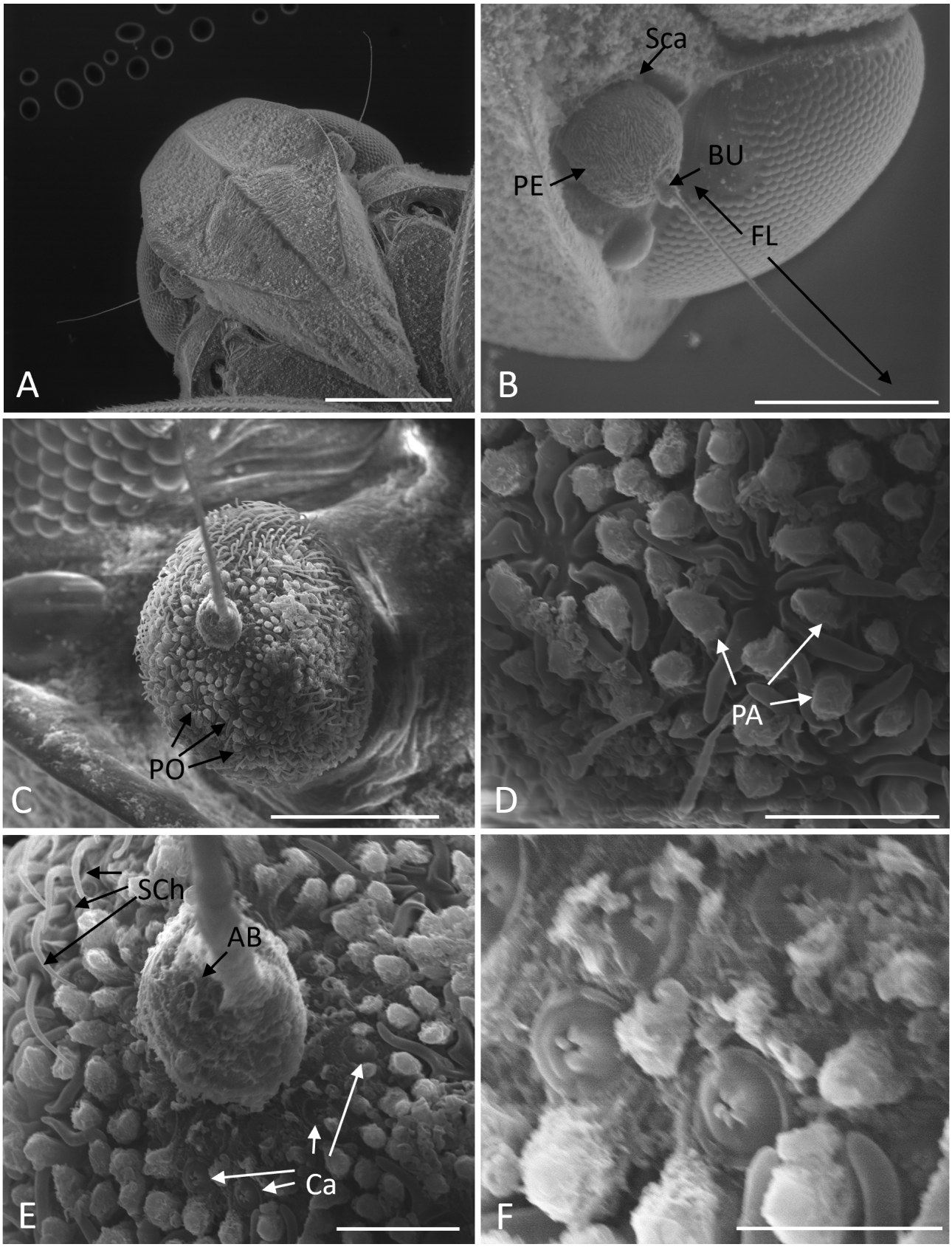

Fig. 3. SEM images of *P. leporinus* (females displayed). A: Distal view of the head capsule with antennae, ×158. B: Flagellum (FL) with bulbus (BU) based on the pedicel (PE), inside the scape (Sca), ×386. C: Pedicel displaying star-shaped plate organs (PO), ×1050. D: Star-shaped plate organs of digitated type, interspersed by papillae (PA), ×5400. E: Campaniform-like sensilla (Ca) close to the base of the bulbus on the pedicel and sensilla chaetica located opposite (SCh), aperture of the Bourgoin's organ (AB) visible on the top of the bulbus, ×3800. F: Close-up of Ca in (E), ×8000. A and B imaged at low vacuum (70 Pa), C to F at high vacuum. Scale bar: A: 500 µm, B: 300 µm, C: 100 µm, D: 20 µm, E: 20 µm, F: 10 µm.

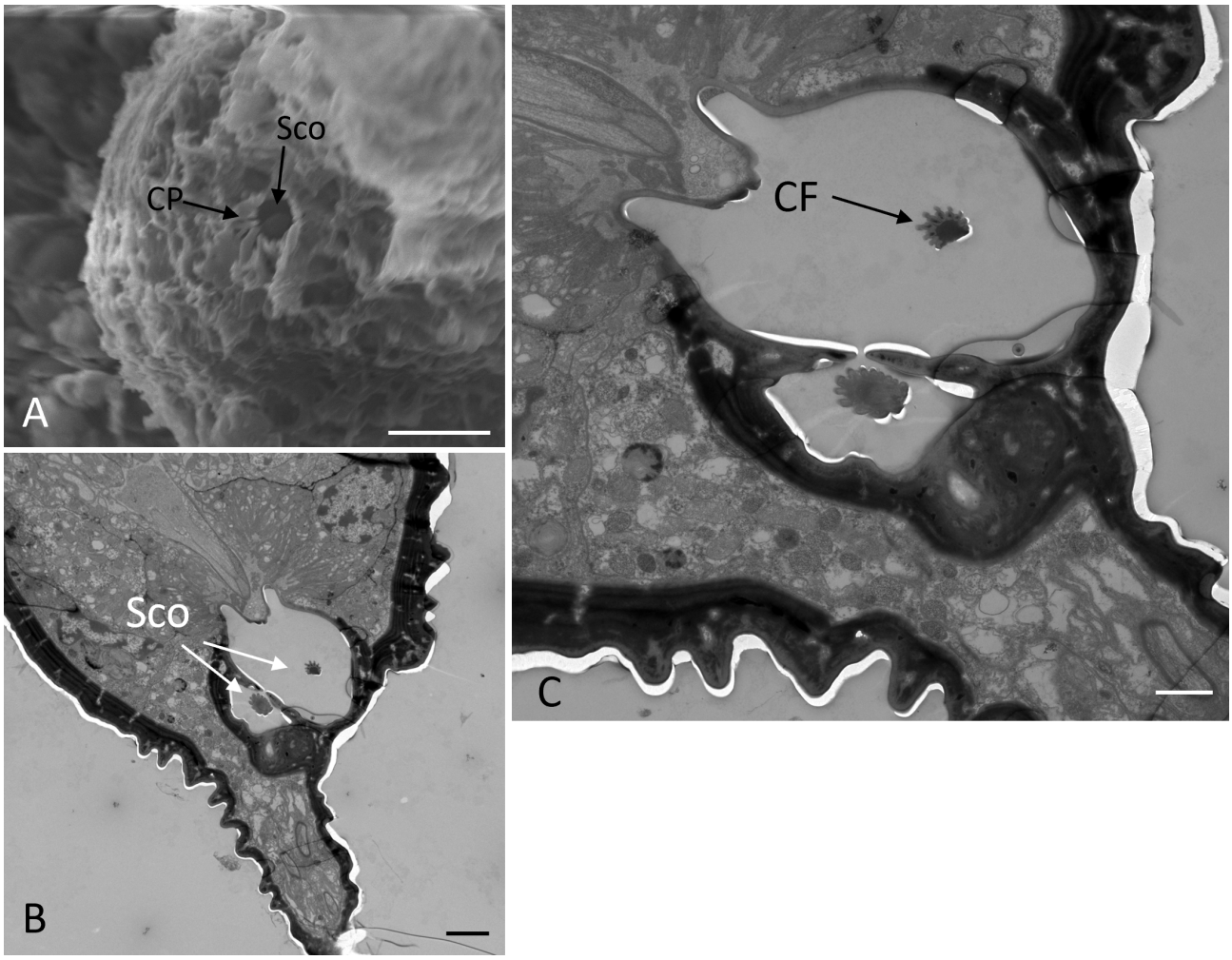

Fig. 4. Electron microscopy images of *P. leporinus* (females displayed). A: (SEM) Close-up of the aperture to the Bourgoin's organ on the bulbus with cuticular processes (CP) and a tip of a sensillum coeloconicum (Sco), ×11980. B: (TEM) Ultrathin section of embedded antenna illustrating the bulbus bearing the Bourgoin's organ with two sensory chambers containing sensilla coeloconica (Sco), ×3000. C: (TEM) Close-up of B) highlighting the pegs of Sco with cuticular fingers (CF) inside, ×7000. Scale-bars: A: 5000 nm, B: 2500 nm, C: 1000 nm.

(estimated mean: 0.048 ± 0.06 SE, p = 0.951, normalised units). Results of the statistical analysis are included in the R code (https://doi.org/10.5073/20260421-161521-0).

3.4 Complex ultrastructure of antennal sensilla

Images of scanning electron microscopy (SEM) and of transmission electron microscopy (TEM) of female and male individuals (3 of each in more detail) of *P. leporinus* were investigated. Visual analysis revealed no sex-specific differences in the types of sensilla found on the antennal surface. However, sample size and resources were too limited to perform a quantitative or statistical analysis of sensillum counts or verify distribution patterns. We classified sensilla based on a classification by Schneider (1964). Figure 3A shows an overview of the location of the antennae on the head capsule of *P. leporinus*.

Antennae of both sexes consist of three parts (Fig. 3B): a thin flagellum which is thickened to a bulbus at its basal end with no sensilla visible on the external surface; the bulbus based on a prominent pedicel which protrudes from a scape hidden in the head capsule below the compound eye in dorsal view. Unlike the flagellum, the pedicel is covered with different types of sensilla indicating distinct functions. On the apical part of the bulbus, a small aperture is visible (Fig. 3E), bearing a chambered cavity with coeloconic sensilla, a typical feature of the Bourgoin organ (Bourgoin, 1985). While in SEM, these sunken organs surrounded by a ring of cuticular projections are merely visible (Fig. 4A), TEM unfolds their complete structure in ultrathin sections of embedded antenna (Fig. 4B, C). On the distal part of the pedicel, round protruding, campaniform-like organs with fine processes surrounding a centric aperture are located close to the base of the bulbus in one or two concentric rows (Fig. 3E, F). Basal to them, flattened, star-shaped plate organs interspersed with domed papillae can be found on the pedicel (Fig. 3D). These organs are lacking towards the base of the bulbus, which is covered by numerous sensilla chaetica (Fig. 3C, E).

In ultrathin sections of the bulbus of a female specimen, two sensory chambers are visible, each of them bearing a peg of corresponding sensilla coeloconica inside (Fig. 4B), as has been described for other planthoppers of the Fulgoromorpha (Bourgoin, 1985; Romani et al., 2009). Both cross-sectioned sensilla pegs have cuticular fingers (Keil,

1999; Romani et al., 2009) and can be classified as specialised types of sensilla coeloconica.

DISCUSSION

This study shows that three VOCs from the wild potato *S. bulbocastanum* are detected by the antennae of *P. leporinus*. At least two of them, nonanal and decanal, are common plant volatiles (Wildt et al., 2003; Karlsson et al., 2009; Feng et al., 2022; Zhou & Jander, 2022) and therefore probably not specific for the observed short-term attractiveness of this planthopper towards the wild potato (Therhaag et al., 2026). For the identification of the third compound, GC-MS/MS analysis would be required, which is unfortunately not available in our lab and represents a limitation of our study. However, the identified two compounds are the most abundant in the volatile composition of *S. bulbocastanum* (Fig. 1).

In the GC-EAD experiments, it is noteworthy that only recordings of male antennae allowed antennal responses to be assigned to specific FID peaks, and the setup was challenging with this planthopper species. This is because the thin flagellum of the antenna easily flipped out of the glass capillary and was highly sensitive to air flow and vibrational disturbances. The antennal preparations of female planthoppers showed an even more variable baseline signal, which may have led to non-reproducible alterations in the antennal signals of females in that setup. To prevent erroneous conclusions being drawn regarding the differences in the receptiveness of male and female antennae, we then investigated the two identified compounds on female antennae further through an EAG experiment. Compared to air, antennae responded significantly to undiluted nonanal and decanal, with nonanal eliciting the most pronounced response, even at lower concentrations of 0.1 and 0.01. Nonanal has a vapour pressure of ~49 Pa at 25°C, decanal ~14 Pa. Using the ideal gas law, the estimated number of molecules per 1 ml puff was $\sim 12 \times 10^{15}$ for nonanal and $\sim 3.3 \times 10^{15}$ for decanal (figures and calculation provided in the Supplementary information). This difference does not scale linearly with the ~2-fold stronger response elicited by nonanal. Although the vapour pressure of the solvent, methanol, was in the same range as that of hexane and substantially higher compared to the aldehydes, its response was not different to that of the air control. A reason for this may be the high polarity of methanol not being able to pass the antennal cuticle as quickly as nonpolar volatiles (Light et al., 1988).

The EAG method was only applied to antennal preparations of females to test the hypothesis that they respond to the same identified compounds as their male counterparts. Therefore, our study does not allow for a comparison of antennal dose-dependent responses between males and females. But as the GC-EAD setup does not produce this kind of distinct puffs of compounds compared to the EAG setup, a lower concentration of stimuli can be assumed in the flow. Thus, a higher sensitivity of antennae from males to both compounds could be hypothesised but would be subject to a comparison by EAG with insects from equal sources. A sex-specific sensitivity could be the case, as Rodrigues et al. (2025) showed that olfactory responses for *Philaenus spumarius* (Linnaeus 1758) to different olive cultivars can vary throughout the life cycle but are also sex-specific. Even olfactory responses to conspecific odours were reported for this species, with a stronger response from males compared to female responses (Sevarika et al., 2022). In our study, we refrain from drawing conclusions about sex-specific antennal sensitivity between experiments as we cannot exclude effects from rearing history, age and prior odour exposure caused by heterogeneous insect sources across them.

This study also investigated, for the first time, the antenna and its ultrastructures of *P. leporinus*. The general antenna structure is similar to those of other planthopper species, with a typical flagellum ending in a bulbus at the base, and the bulbus being connected to a pedicel that itself is based in a scape which barely protrudes from the head capsule. Compared to other hemipteran species of the Auchenorrhyncha, the scape of *P. leporinus* is rather inconspicuous and located behind the compound eye, similar to a related species, the cixiid planthopper *Hyalesthes obsoletus* (Signoret, 1865) (Romani et al., 2009), but unlike the Australian cixiid *Tyligma* gen. n., which has a prominent scape (Löcker & Holzinger, 2020). Another feature of *P. leporinus* that is characteristic of fulgoromorph planthoppers is the absence of sensilla on the flagellum, whereas the sensory surface of the pedicel is covered by different specified putatively chemoreceptive and tactile sensilla. Although we can conclude from the GCEAD and EAG experiments that *P. leporinus* responds to volatile compounds, we cannot assign the electrophysiological responses to specific sensilla observed but rather hypothesise their likely function. Compounds would need to be directed onto the different sensilla for a proof. This also applies to the sensilla coeloconica which are located inside the Bourgoin's organ (Bourgoin, 1985), its aperture visible on the bulbus of *P. leporinus*. For *H. obsoletus*, Romani et al. (2009) assumed that one of the sensilla inside this organ is for the perception of CO_2, the other for thermo- and olfactory reception. Bearing in mind that "microscopic identity does not prove functional identity" as emphasized by Schneider (1964), we resist speculating on their functional purpose at this stage of investigation. *P. leporinus* also exhibits flattened star-shaped plate organs on the pedicel, which have been reported for *Meenoplus* spp. (Hemiptera: Auchenorrhyncha) (Remane & Wachmann, 1993; Hoch et al., 2021), and other planthoppers of the fulgoromorph families Meenoplidae, Kinnaridae and Achilixiidae, and which are suggested to be complex olfactory organs (Bourgoin & Deiss, 1994).

In our study, we did not discover sex-specific differences of the antennal structure of *P. leporinus*, or its sensilla types, likewise to its cixiid relative, *H. obsoletus* (Romani et al., 2009). Given the limited specimens examined, our observations are rather qualitative than quantitative and represent a preliminary description which could stimulate further, more detailed investigations.

From the perspective of applied entomology and biological vector control, our results may be a first step, but further investigations on antennal reactions to plant or conspecific compounds would be required.

DATA AVAILABILITY STATEMENT. Data are available from the OpenAgrar Repository: https://doi.org/10.5073/20260421-161521-0.

ACKNOWLEDGEMENTS. We would like to thank C. Gerbert for her excellent insect rearing, F. Hergenhahn for his assistance in the greenhouse, and to S. Kugler for her assistance in catching plant hoppers and the setup for GC-EAD. We are grateful for inputs from A. Jürgens related to GCEAD result display, EAG response calculation and the discussion. We also thank B. Czarnobai and J. Gallinger for technical exchange on the GC-EAD software settings, A. Karimi and A. Koßmann for support in the AMDIS analysis, and S. Stein for measuring GC-MS samples and hardware maintenance. For the work conducted by E. Therhaag, the study received funds from the project SIKAZIKA, funded by the European Union and the State Hesse, Germany within the framework of the European innovation partnership for agricultural productivity and sustainability (EIP-Agri, grant number 9100443-INVEST-1).

REFERENCES

Behrmann S.C., Rinklef A., Lang C., Vilcinskas A. & Lee K.-Z. 2023: Potato (*Solanum tuberosum*) as a new host for *Pentastiridius leporinus* (Hemiptera: Cixiidae) and *Candidatus* Arsenophonus phytopathogenicus. — *Insects* **14**: 281, 13 pp.

Bourgoin T. 1985: Morphologie antennaire des *Tettigometridae* (Hemiptera, Fulgoromorpha). — *Nouv. Rev. Entomol.* **1**: 11–20.

Bourgoin T. & Deiss V. 1994: Sensory plate organs of the antenna in the *Meenoplidae-Kinnaridae* group (Hemiptera: Fulgoromorpha). — *Int. J. Insect Morphol. Embryol.* **23**: 159–168.

Bozzola J.J. 2014: Conventional specimen preparation techniques for scanning electron microscopy of biological specimens. In Kuo J. (ed.): *Electron Microscopy: Methods and Protocols*. Humana Press, Totowa, NJ, pp. 133–150.

Duduk B., Ćurčić Ž., Stepanović J., Böhm J.W., Kosovac A., Rekanović E. & Kube M. 2023: Prevalence of a '*Candidatus* Phytoplasma solani' – related strain designated as new 16SrX-II-P subgroup over '*Candidatus* Arsenophonus phytopathogenicus' in sugar beet in Eastern Germany. — *Plant Dis.* **107**: 3792–3800.

EPPO 2023: PM 4/28 (2) Certification scheme for seed potatoes. — *EPPO Bull.* **53**: 460–475.

Faal H., Canlas I.J., Cossé A., Jones T.H., Carrillo D. & Cooperband M.F. 2023: Investigating photo-degradation as a potential pheromone production pathway in spotted lanternfly, *Lycorma delicatula*. — *Insects* **14**: 551, 17 pp.

Feng H., Gou C., Aimaiti D., Sun P., Wang L. & Hao H. 2022: Plant volatile organic compounds attractive to *Lygus pratensis*. — *Open Life Sci.* **17**: 362–371.

Griffin B.J. 2007: Variable pressure and environmental scanning electron microscopy. In Kuo J. (ed.): *Electron Microscopy: Methods and Protocols*. Humana Press, Totowa, NJ, pp. 467–495.

Gross J., Gallinger J. & Rid M. 2019: Collection, identification, and statistical analysis of volatile organic compound patterns emitted by *Phytoplasma* infected plants. In Musetti R. & Pagliari L. (eds): *Phytoplasmas: Methods and Protocols*. Springer, New York, NY, pp. 333–343.

Hoch H., Sendra A., Montagud S., Teruel S. & Lopes Ferreira R. 2021: First record of a cavernicolous *Kinnaridae* from the Old World (Hemiptera, Auchenorrhyncha, Fulgoromorpha, Kinnaridae, Adolendini) provides testimony of an ancient fauna. — *Subterr. Biol.* **37**: 1–26.

Karimi A. & Gross J. 2024: Development and validation of an innovative headspace collection technique: volatile organic compound patterns emitted by different developmental stages of *Halyomorpha halys*. — *Front. Hortic.* **3**: 1380008, 10 pp.

Karlsson M.F., Birgersson G., Cotes Prado A.M., Bosa F., Bengtsson M. & Witzgall P. 2009: Plant odor analysis of potato: Response of Guatemalan moth to above- and belowground potato volatiles. — *J. Agric. Food Chem.* **57**: 5903–5909.

Keil T.A. 1999: Morphology and development of the peripheral olfactory organs. In Hansson B.S. (ed.): *Insect Olfaction*. Springer, Berlin, Heidelberg, pp. 5–47.

Kuznetsova A., Brockhoff P.B., Christensen R.H.B. & Jensen S.P. 2026: *lmerTest: Tests in Linear Mixed Effects Models.* URL: https://cran.r-project.org/web/packages/lmerTest/index.html.

Lang C., Dettweiler A., Benaouda S., Kreimer D., Löffler D., Glaser E., Adam H. & Bojanowicz S.L. 2025: *Pentastiridius leporinus* as a plant disease vector: The practical state of knowledge and derived research objectives. — *Sugar Ind. Int.* **150**: 105–120.

Lenth R.V., Piaskowski J., Banfai B., Bolker B., Buerkner P., Giné-Vázquez I., Hervé M., Jung M., Love J., Miguez et al. 2026: *emmeans: Estimated Marginal Means, aka Least-Squares Means*. URL: https://cran.r-project.org/web/packages/emmeans/index.html.

Lenz M.-S., Müller S., Gäbelein R., Meiners T., Böttcher C. & Gorzolka K. 2025: Bioactivity of acyl solamines from leaves of *Solanum bulbocastanum* against *Alternaria solani* and *Botrytis cinerea*. — *Potato Res.* **68**: 4077–4097.

Light D.M., Jang E.B. & Dickens J.C. 1988: Electroantennogram responses of the mediterranean fruit fly, *Ceratitis capitata*, to a spectrum of plant volatiles. — *J. Chem. Ecol.* **14**: 159–180.

Löcker B. & Holzinger W.E. 2020: *Tyligma* gen. nov., a new Australian genus of planthopper and a key to the Australian genera of Cixiini (Hemiptera: Cixiidae). — *Aust. Entomol. Soc.* **59**: 747–757.

Mahillon M., Bussereau F., Dubuis N., Brodard J., Debonneville C. & Schumpp O. 2025: First detection of *Arsenophonus* in potato crop in Switzerland: A threat for the processing industry? — *Potato Res.* **68**: 2567–2578.

Product Data Sheet – SilFlow® GC 4 Port Splitter 2022: *PD-1079-G_RevE © Trajan Scientific and Medical 02/2022.* URL: https://www.trajanscimed.com/products/pd-1079-g (last accessed 24 Apr. 2026).

Remane R. & Wachmann E. 1993: *Zikaden kennenlernen, beobachten*. Naturbuch Verlag, Augsburg, 288 pp.

Ren L.L., Balakrishnan K., Luo Y.Q. & Schütz S. 2017: EAG response and behavioral orientation of *Dastarcus helophoroides* (Fairmaire) (Coleoptera: Bothrideridae) to synthetic host-associated volatiles. — *PLoS ONE* **12**: e0190067, 18 pp.

Richert-Pöggeler K.R., Franzke K., Hipp K. & Kleespies R.G. 2019: Electron microscopy methods for virus diagnosis and high resolution analysis of viruses. — *Front. Microbiol.* **9**: 3255, 8 pp.

Rid M., Markheiser A., Stein S., Hoffmann C. & Gross J. 2019: Volatiles of several grapevine cultivars emitted at different phenological stages linked to discriminatory ability of grapevine moths. — *J. Plant Dis. Prot.* **126**: 115–127.

Rodrigues I., Benhadi-Marín J., Rodrigues N., Baptista P. & Pereira J.A. 2025: Seasonal olfactory response of *Philaenus spumarius* (Hemiptera: Aphrophoridae) towards traditional Portuguese olive cultivars. — *Crop Prot.* **197**: 107367, 11 pp.

Romani R., Rossi Stacconi M.V., Riolo P. & Isidoro N. 2009: The sensory structures of the antennal flagellum in *Hyalesthes obsoletus* (Hemiptera: Fulgoromorpha: Cixiidae): A functional reduction? — *Arthropod Struct. Dev.* **38**: 473–483.

Schneider D. 1964: Insect antennae. — *Annu. Rev. Entomol.* **9**: 103–122.

Sémétey O., Bressan A., Richard-Molard M. & Boudon-Padieu E. 2007: Monitoring of proteobacteria and phytoplasma in sugar beets naturally or experimentally affected by the disease syndrome 'Basses richesses'. — *Eur. J. Plant Pathol.* **117**: 187–196.

Sevarika M., Rondoni G., Ganassi S., Pistillo O.M., Germinara G.S., De Cristofaro A., Romani R. & Conti E. 2022: Behavioural and electrophysiological responses of *Philaenus spumarius* to odours from conspecifics. — *Sci. Rep.* **12**: 8402, 8 pp.

Syntech 2004: *Electroantennography – A Practical Introduction.* Syntech Ltd., Hilversum, 29 pp.

Therhaag E., Schneider B., Zikeli K., Maixner M. & Gross J. 2024a: *Pentastiridius leporinus* (Linnaeus, 1761) as a vector of phloem-restricted pathogens on potatoes: '*Candidatus* Arsenophonus phytopathogenicus' and '*Candidatus* Phytoplasma solani.' — *Insects* **15**: 189, 11 pp.

Therhaag E., Ulrich R., Gross J. & Schneider B. 2024b: Onion (*Allium cepa*) as a new host for '*Candidatus* Arsenophonus phytopathogenicus' in Germany. — *Plant Dis.* **108**: 2914, 1 p.

Therhaag E., Gorzolka K. & Gross J. 2026: Lethal effects of the wild potato *Solanum bulbocastanum* on the planthopper *Pentastiridius leporinus*, a vector of bacterial pathogens in potato. — *J. Appl. Entomol.* **150**: 756–769.

Wildt J., Kobel K., Schuh-Thomas G. & Heiden A.C. 2003: Emissions of oxygenated volatile organic compounds from plants. Part II: Emissions of saturated aldehydes. — *J. Atmospheric Chem.* **45**: 173–196.

Witczak N., Benaouda S., Wahl F., Göbbels H., Lang C., Jarausch B. & Maixner M. 2025: Carrot (*Daucus carota* L.) as host for *Pentastiridius leporinus* and phloem-restricted pathogens in Germany. — *Biology* **14**: 1152, 16 pp.

Witczak N., Benaouda S., Ritz J., Wahl F., Lang C., Maixner M. & Markheiser A. 2026: First Report of 16SrXII-P related phytoplasma in asparagus (*Asparagus officinalis*) and rhubarb (*Rheum rhabarbarum*) in Germany. — *Plant Dis.* **110**: 1984, 1 p.

Zhou S. & Jander G. 2022: Molecular ecology of plant volatiles in interactions with insect herbivores. — *J. Exp. Bot.* **73**: 449–462.

Received April 24, 2026; revised and accepted July 29, 2026
Published online August 11, 2026

Supplementary information

Calculation. The vapour pressure p (in Pascal) of the substances nonanal and decanal is different and consequently results in a different number of molecules (stimuli) per puff volumina V_{puff}. Nonanal has a vapour pressure of ~49 Pa at 25°C, decanal ~14 Pa. Using the ideal gas law, the estimated number of molecules per 1 ml puff was $\sim 12 \times 10^{15}$ for nonanal and $\sim 3.3 \times 10^{15}$ for decanal.

The calculation was performed in two steps, for both nonanal and decanal, with V_{puff} set to 1 mL (1×10^{-6} m³). First, the amount of substance n_{puff}, for each compound, in the vapour with R being the gas constant (8.314 J mol^{-1} K^{-1}) and T, the absolute temperature in Kelvin, was calculated:

$$n_{puff} = \frac{p \times V_{puff}}{R \times T} \quad (1)$$

In the second step, we multiplied the result (n_{puff}) with the Avogadro constant N_A ($6.02214076 \times 10^{23}$mol^{-1}) to derive the number of molecules N from the amount of substance n, making use of the formula:

$$N = n \times N_A \quad (2)$$

$$N_{puff} = n_{puff} \times N_A \quad (3)$$

Results for all compounds, including the positive control (hexane) and the solvent control (methanol) are displayed in Table S1.

Table S1. Selected synthetic compounds used as olfactory stimuli in the EAG experiments tested on female adult planthoppers of *P. leporinus*.

Compound	Purity	Source	Vapour pressure [a] (mmHG at 25°C) in Pa	N_{puff} [b] (molecules per puff)
Decanal	≥99%	Sigma Aldrich	(0.103), ~13.73	$\approx 3.3 \times 10^{15}$
Nonanal	≥95%	Sigma Aldrich	(0.37), ~49.33	$\approx 12 \times 10^{15}$
Methanol	≥99.9%	Sigma Aldrich	(127), ~16931.94	$\approx 4113 \times 10^{15}$
Hexane	≥99%	Sigma Aldrich	(135), ~17998.52	$\approx 4373 \times 10^{15}$

Sigma Aldrich Chemie GmbH, Taufkirchen, Germany. [a] Values in the table derived from PubChem, Hazardous Substances Data Bank. [b] Puff set to 1 mL, for ease of calculation.